NJC

PAPER

View Article Online
View Journal

Cite this: DOI: 10.1039/c8nj04695f

An ESIPT based chromogenic and fluorescent ratiometric probe for Zn^{2+} with imaging in live cells and tissues†

Saswati Gharami,[a] Krishnendu Aich,[a] Deblina Sarkar,‡[b] Paramita Ghosh,[b] Nabendu Murmu*[b] and Tapan Kumar Mondal*[a]

Received 14th September 2018,
Accepted 14th December 2018

DOI: 10.1039/c8nj04695f

rsc.li/njc

A new ESIPT based fluorescent probe has been introduced for selective detection of Zn^{2+} in human breast cancer cells. The designed probe exhibits a prominent ratiometric fluorescence change along with a sharp blue shift of ~71 nm which can be attributed to the hampering of the ESIPT process. The probe is efficient enough to detect Zn^{2+} solely in the presence of other biologically relevant cations with a limit of detection value of 1.6×10^{-7} M. The experimentally observed changes in the structure and absorption properties of the probe after complete addition of Zn^{2+} were further studied by density functional theory (DFT) and time dependent density functional theory (TDDFT) calculations. Moreover, the dip-stick experiment with this probe displays both absorption and fluorescence color changes after exposure to Zn^{2+} which also turns out to be a potential application for the probe. Live cell imaging studies have been carried out using human breast cancer cells (MCF-7) and tissues.

Introduction

Rapid and selective recognition of ions in aqueous media has become a vital part of research currently. This is very much needed in order to protect the environment, to monitor all the biological processes and also for identification of several diseases. Among an array of detection methods, the fluorescence based sensing technique has been proved to be of immense importance due to its simplicity, sensitivity, high degree of specificity, low detection limit, cost-effectiveness and short response time.[1] To date several fluorescent chemosensors have been developed for detecting many metal cations.[2] Zinc is the second most abundant transition metal in the human body after iron and it is also an essential trace mineral comprising more than 250 metalloenzymes.[3] There are several different biological functions where dependency on zinc is very much desired such as our immune system functions, DNA synthesis, neural signal transmission, apoptosis regulation, mammalian reproduction, cellular transport, metabolism and overall growth of the human body.[4] Zinc actively participates in various biological processes such as oxygen transport,[5] gene expression[6] and cellular metabolism.[7] But the discrepancy of zinc ion concentration in the human body may lead to several life alarming diseases such as Alzheimer's disease,[8] epilepsy,[9] ischemic stroke,[10] prostate cancer[11] and Parkinson's disease.[12] Zinc is also a harmful environmental pollutant.[13] Hence there is an urgent need to develop chemosensors for the efficient detection of zinc, both '*in vivo*' as well as '*in vitro*'. The difficulty in sensing zinc distinctly in some intricate biological systems is attributed to the fact that zinc ions are silent to some common analytical techniques like Mossbauer, NMR and electron paramagnetic resonance (EPR) compared to other transition metal ions. Thus the detection of zinc with the help of fluorescent chemosensors is now a widely popular area of research. Due to the huge demand, several sensing devices involving different Schiff's bases, polythiacrown ethers, *etc.* have been developed in the past few years,[14] although most of them have the drawback of inadequate selectivity towards Zn^{2+} due to special interference from Cd^{2+} ions.[15] To date, many zinc sensors have been reported,[16] and a few of them show ratiometric fluorescence response. Despite of those nicely designed probes, there is still a great need to fabricate new ratiometric fluorescent probes which can selectively detect Zn^{2+} in environmental as well as biological samples.

Herein a new fluorescent chemosensor (HBS) has been introduced which selectively binds to Zn^{2+} over other metal cations with high sensitivity. The probe shows a profound ratiometric change in the emission spectra upon addition of Zn^{2+}. The probe, HBS, can also detect Zn^{2+} in live human breast cancer cells and

[a] *Department of Chemistry, Jadavpur University, Kolkata-70003, India. E-mail: tapank.mondal@jadavpuruniversity.in*
[b] *Department of Signal Transduction and Biogenic Amines (STBA), Chittaranjan National Cancer Institute, Kolkata-700026, India*

† Electronic supplementary information (ESI) available. See DOI: 10.1039/c8nj04695f

‡ Present address: Department of Chemistry, Bagnan College, Howrah, WB 711303, India.

tissues. Further DFT and TDDFT calculations are used to interpret the sensing mechanism of HBS towards Zn^{2+}.

Experimental

Materials and methods

All the organic chemicals and inorganic materials used for this study were purchased from commercial suppliers. ^{1}H and ^{13}C NMR spectra were recorded on a Bruker 300 MHz instrument in DMSO-d_6 solvent using TMS as an internal standard. HRMS spectra were recorded on a Waters (Xevo G2 Q-Tof) mass spectrometer. UV-vis spectra were recorded on a Perkin-Elmer Lambda 750 spectrophotometer whereas the fluorescence properties were investigated using a Shimadzu RF-6000 fluorescence spectrophotometer at room temperature (298 K). Thin layer chromatography (TLC) was carried out on Merck 60 F_{254} plates with a thickness of 0.25 mm. Fluorescence lifetimes were measured using a time-resolved spectrofluorometer from IBH, UK.

General method of UV-vis and fluorescence titrations

UV-Vis method. For UV-vis titrations, a stock solution of the receptor (10 μM) was prepared in [(MeOH/H_2O), 1/1, v/v] (at 25 °C) solution using HEPES buffer. The solutions of the guest cations using their chloride salts were prepared in deionized water using HEPES buffer at pH = 7.2 in the order of 1×10^{-5} M. Solutions of a variety of concentrations containing the probe and increasing concentrations of cations were prepared individually. The spectra of these solutions were recorded by means of a UV-vis method.

Fluorescence method. For fluorescence titrations, the stock solution of the probe (10 μM) was the same as that used for UV-vis titration. The solutions of the guest cations using their chloride salts in the order of 1×10^{-5} M were prepared in deionised water similarly. Solutions of different concentrations containing the probe and increasing concentrations of cations were prepared separately and the spectra of these solutions were recorded by means of a fluorescence method.

Synthetic procedure of the probe (HBS)

To the suspension of compound **2** (0.03 g, 0.152 mmol) in ethanol, 2-hydroxybenzohydrazide (0.05 g, 0.255 mmol) was added with continuous stirring. The reaction mixture was then refluxed for 7 hours. After ensuring the completion of the reaction, the reaction mixture was allowed to cool to room temperature. After cooling at room temperature, the solvent was evaporated under reduced pressure and water (10 ml) was added to the crude product and then extracted using dichloromethane (3 × 20 ml). Then the DCM portion was dried over anhydrous sodium sulphate and evaporated. The evaporation of the solvent under reduced pressure affords a light yellow solid compound which was further purified through column chromatography using dichloromethane as the eluent. Yield is 0.063 g; 83%.

^{1}H NMR (300 MHz, DMSO-d_6). δ 6.99 (t, J = 8.7 Hz, 3H), 7.17 (t, J = 7.0 Hz, 1H), 7.45 (t, J = 7.0 Hz, 3H), 7.54 (d, J = 7.5 Hz, 1H), 7.77 (d, J = 7 Hz, 1H), 7.88 (d, J = 7.4 Hz, 1H), 8.07 (d, J = 7.8 Hz, 1H), 8.16 (d, J = 7.6 Hz, 1H), 8.37 (d, J = 7.8 Hz, 1H), 8.77 (s, 1H), 11.81 (s, 1H), 13.50 (s, 1H).

^{13}C NMR (150 MHz, DMSO-d_6). δ 116.2, 117.8, 119.5, 120.1, 120.4, 122.5, 122.7, 125.6, 126.9, 129.3, 130.9, 133.2, 134.5, 135.2, 149.0, 151.8, 156.5, 159.2, 159.4, 163.8, 164.9.

HRMS (ESI, positive). Calcd for $C_{21}H_{16}N_3O_3S$ $[M + H]^+$ (m/z): 390.0912; found: 390.1196.

Synthesis of Zn^{2+} complex (HBS–Zn^{2+}) of the probe

The probe HBS (62 mg) and $ZnCl_2$ (22 mg) were mixed together and dissolved in 7 ml of acetonitrile. After reflux for 6 hours the reaction mixture was cooled to room temperature. An orange coloured precipitate was obtained which was filtered and dried in vacuum.

HRMS (ESI, positive). Calcd for $C_{21}H_{12}ClN_3NaO_3SZn$ $[M + Zn^{2+} + Cl^- + Na^+ - H]^+$ (m/z): 507.9477; found: 507.2065.

Synthetic procedure of the analogue (HBB)

Benzohydrazide (0.10 g, 0.735 mmol) and compound **2** (0.19 g, 0.735 mmol) were mixed together using methanol as solvent in a round-bottomed flask followed by reflux for 3 hours. After cooling the reaction mixture to room temperature, a white precipitate was obtained which was filtered followed by washing with cold methanol and dried to yield the desired solid product. Yield is 0.219 g; 80%.

^{1}H NMR (300 MHz, DMSO-d_6). δ 7.17 (t, J = 7.5 Hz, 1H), 7.46 (t, J = 7.0 Hz, 1H), 7.57 (d, J = 6.9 Hz, 3H), 7.62 (d, J = 7.0 Hz, 1H), 7.78 (d, J = 6.7 Hz, 2H), 7.96 (d, J = 6.9 Hz, 1H), 8.08 (d, J = 7.6 Hz, 1H), 8.17 (d, J = 7.4 Hz, 1H), 8.38 (d, J = 7.8 Hz, 1H), 8.74 (s, 1H), 12.39 (s, 1H), 13.56 (s, 1H).

^{13}C NMR (100 MHz, DMSO-d_6). δ 119.7, 119.9, 122.0, 122.3, 125.3, 126.5, 127.7, 128.6, 130.4, 132.9, 134.9, 147.9, 155.9, 159.2, 162.8.

HRMS (ESI, positive). Calcd for $C_{21}H_{16}N_3O_2S$ $[M + H]^+$ (m/z): 374.0963; found: 374.1011 and for $C_{21}H_{15}N_3NaO_2S$ $[M + Na]^+$ (m/z): 396.0783; found: 396.0781.

Computational method

Full geometry optimizations were carried out using the density functional theory (DFT) method at the B3LYP[17–20] level for the compounds. The 6-31+G(d) basis set was used for all elements except zinc. The LanL2DZ basis set with the effective core potential (ECP) set of Hay and Wadt[21] was used for the Zn^{2+} complex. The vibrational frequency calculations were performed to ensure that the optimized geometries represent the local minima and there were only positive eigenvalues. Vertical electronic excitations based on B3LYP optimized geometries were computed using the time-dependent density functional theory (TDDFT) formalism[22–24] in methanol using the conductor-like polarizable continuum model (CPCM).[25–27] All calculations were performed with the Gaussian 09 program package[28] with the aid of the GaussView visualization program.

Live cell imaging study

Breast cancer cell line. MCF-7 cells were grown on 22 × 22 mm glass cover slips placed at the bottom of six well plates

and treated with chemosensor (HBS) and HBS–Zn^{2+} complex (15 μM each) for 1 h. Cells were then fixed with methanol and washed with 0.5% phosphate buffer saline tween (PBST) twice and 1× PBS thrice. The cover slips were mounted on a glass slide and were observed under a fluorescence microscope (Leica DM4000 B, Germany) at 20× magnification.

Breast cancer tissue sample. Tissue samples from breast cancer patients were obtained from Chittaranjan National Cancer Hospital, Kolkata, India, and fixed in formalin overnight. Paraffin blocks of the fixed tissues were prepared using the standard protocol.[29] Tissue blocks embedded in the blocks were then cut into a desired thickness of 3 micron using a microtome and fixed onto the poly L-lysin coated slides. Slides were deparaffinized and rehydrated and finally washed with phosphate buffer saline Tween (PBS-T) for 10 minutes. Tissue sections were incubated with each chemosensor (HBS) and HBS–Zn^{2+} complex (15 μM each) for 1 h. After incubation, the breast cancer tissues were washed with PBS-T solution for 10 minutes and stained with DAPI (1 : 100) for 30 seconds. Slides were mounted with glycerol and observed under a fluorescence microscope (Leica DM4000 B, Germany) at 20× magnification.

Results and discussion

Design and synthesis

The synthetic procedures of the probe (HBS) and the analogue (HBB) are shown in Scheme 1. 2-Hydroxybenzohydrazide (**1**),[30] 3-(benzo[*d*]thiazol-2-yl)-2-hydroxybenzaldehyde (**2**)[31,32] and benzohydrazide (**3**)[33] were synthesized according to reported procedures. Reflux condensation of compound **2** and compound **1** in ethanol for about 10 hours affords the desired probe (HBS) with a high yield (0.065 g, 86%). Similarly, the analogous compound (HBB) was fabricated *via* the reflux condensation of compounds **2** and **3** in methanol solvent for 3 hours. The yield of HBB is found to be 80%. The ^{1}H and ^{13}C NMR spectra of the probe (HBS) and the analogue (HBB) are shown in the ESI along with their HRMS spectra (Fig. S10–S15, ESI†).

Cation sensing studies

UV-Vis study

In UV-vis, the receptor, HBS, exhibits absorbance bands at 295 nm and 345 nm along with a shoulder band at 424 nm in MeOH/H_2O (1/1, v/v, 10 mM HEPES buffer, pH = 7.2). Upon gradual addition of Zn^{2+} (40 μM) to the receptor solution the band at 345 nm shows a decrease in absorption intensity and a new band appears at 416 nm with the formation of isosbestic points at 330 nm and 381 nm respectively (Fig. 1). The UV-vis spectrum of HBSA is also studied in the presence of other metal ions *i.e.*, Na^{+}, K^{+}, Ca^{2+}, Mg^{2+}, Mn^{2+}, Fe^{3+}, Cr^{3+}, Al^{3+}, Co^{2+}, Ni^{2+}, Cu^{2+}, Cd^{2+} and Hg^{2+} but there is hardly any change in the spectral pattern (Fig. S1, ESI†).

The absorption spectrum of the newly designed analogue (HBB) is also studied. The absorbance band at 297 nm is observed along with a band at 353 nm and a slight shoulder at 421 nm in MeOH/H_2O (1/1, v/v, 10 mM HEPES buffer, pH = 7.2). Upon addition of Zn^{2+} (40 μM) into the solution of HBB, the band at 353 nm diminishes while the absorbance of the band at 421 nm increases and generates a new band with maxima at 418 nm. Two isosbestic points at 335 nm and 379 nm are noticed respectively (Fig. S2, ESI†).

Fluorescence studies. The emission spectra of HBS and its fluorescence titration with Zn^{2+} were also recorded in MeOH/H_2O (1/1, v/v, 10 mM HEPES buffer, pH = 7.2) solution. In the absence of any metal free receptor HBS exhibits a strong emission band at 549 nm with a small hump at 481 nm upon excitation at 380 nm. Gradual addition of Zn^{2+} to HBS solution results in a sharp ratiometric increase in fluorescence intensity with blue shifting of the band at 478 nm while the band at 549 nm disappears (Fig. 2). This change may be attributed to the ESIPT process.

We have also studied the emission properties of the analogue (HBB) to compare with those of HBS. The fluorescence studies were performed in the same solvent *i.e.*, MeOH/H_2O (1/1, v/v, 10 mM HEPES buffer, pH = 7.2). Free HBB shows an emission peak at 555 nm along with a slight hump at 478 nm (λ_{ex} = 355 nm). Due to the presence of Zn^{2+} (40 μM) in this solution there was a decrease in the emission band at 555 nm to 540 nm whereas the band at 478 nm increases slightly and shifts to 480 nm (Fig. S3, ESI†). The sharp ratiometric change which was observed in the emission profile of HBS after addition of Zn^{2+} is clearly missing here. Even after further addition of Zn^{2+} into the solution of HBB, the emission intensity at 480 nm was not increased as effectively as in the case of HBS. From these

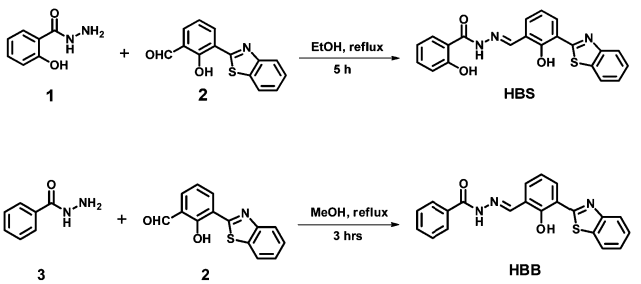

Scheme 1 Synthesis of the probe (HBS) and its analogous compound (HBB).

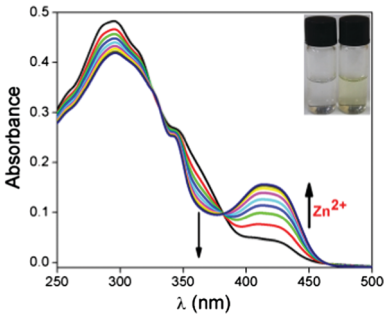

Fig. 1 Change of absorption spectra of HBS (10 μM) upon gradual addition of Zn^{2+} (0 to 40 μM). Inset: Photograph showing the visible color change of HBS before and after addition of Zn^{2+} (40 μM).

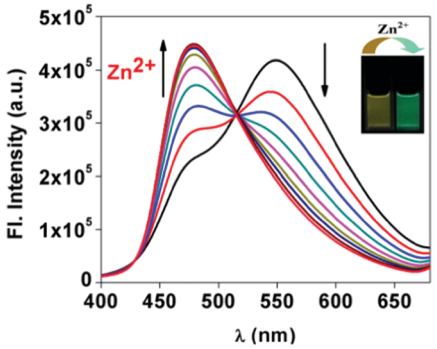

Fig. 2 Change of emission spectra of HBS (10 μM) upon gradual addition of Zn^{2+} (0 to 20 μM). Inset: Visible emission observed from HBS in the absence and presence of 40 μM of Zn^{2+}, under UV light.

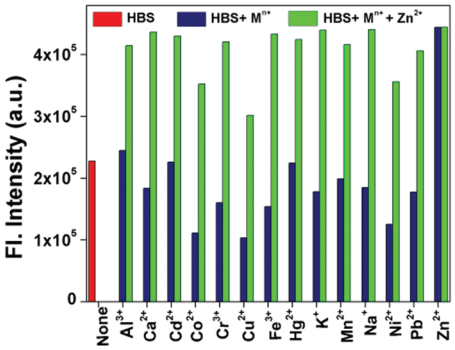

Fig. 3 Competition study using a fluorescence method after addition of different analytes (40 μM) in HBS solution (10 μM) in the presence of Zn^{2+} (40 μM).

emission studies, we can conclude that the probe HBS is a more efficient sensor for Zn^{2+} compared to its analogue, HBB. So, we have chosen HBS to perform further studies with Zn^{2+} as well as for its applications *via* live cell and tissue imaging.

A mole-ratio plot obtained from fluorescence titration indicates that the receptor shows an increase in emission intensity till the ratio of HBS : Zn^{2+} reaches ~1, after that there is hardly any increase in the emission intensity (Fig. S4, ESI†). In order to quantify the stoichiometry of the complex of HBS with Zn^{2+}, Job's plot analysis was carried out. The maxima appears at a mole fraction of 0.5 for the HBS–Zn^{2+} complex which corresponds to the 1 : 1 complex formation of HBS with Zn^{2+} (Fig. S5, ESI†). From the emission spectral change, the limit of detection of the probe HBS with Zn^{2+} was determined using the equation LOD = $K \times SD/S$ where 'SD' is the standard deviation of the blank solution and '*S*' in the slope of the calibration curve (Fig. S6, ESI†). The limit of detection is found to be 1.6×10^{-7} M for Zn^{2+}. This result clearly demonstrates that this synthesized probe is highly efficient in sensing Zn^{2+} even at very minute levels. From fluorescence titration, the association constant of HBS with Zn^{2+} is found to be 1.6×10^{5} M^{-1} from the Benesi–Hildebrand plot (Fig. S7, ESI†), which indicates that the HBS–Zn^{2+} complex is sufficiently stable. To understand the excited state stability, the luminescence lifetime measurements were also carried out. The lifetime decays of the free receptor (HBS) and the HBS–Zn^{2+} complex fit well with the bi-exponential decay curve and the lifetime of HBS (1.73 ns) is significantly decreased in the presence of Zn^{2+} (0.82 ns) (Fig. S8, ESI†).

The emission spectra of HBS (10 μM) were also recorded in the presence of other metal cations *i.e.*, Na^{+}, K^{+}, Ca^{2+}, Mg^{2+}, Mn^{2+}, Cu^{2+}, Fe^{3+}, Cr^{3+}, Co^{2+}, Ni^{2+}, Al^{3+}, Cd^{2+} and Hg^{2+} (10 μM) in MeOH/H_2O (1/1, v/v, 10 mM HEPES buffer, pH = 7.2) but there is hardly any change in the emission intensity of HBS (Fig. S9, ESI†). In order to study the selectivity of HBS towards Zn^{2+}, interference experiment was carried out by measuring the emission intensity of HBS (10 μM) in the presence of other cations. It is observed that other metal ions do not cause any significant interference for Zn^{2+} (Fig. 3).

Mechanism of Zn^{2+} sensing

The enhancement in the fluorescence intensity of HBS after addition of Zn^{2+} is possibly attributed to a very important mechanism named ESIPT (excited state intramolecular proton transfer).[34,35] At first, HBS itself exhibits strong fluorescence intensity as ESIPT was on as the transferable hydrogen remains free and can be transferred to give two desired tautomers (Fig. 4). But after introduction of Zn^{2+}, the exchange of that transferrable hydrogen was inhibited as Zn^{2+} binds to the probe HBS thereby switching off the ESIPT process which accounts for the blue shift of ~69 nm.

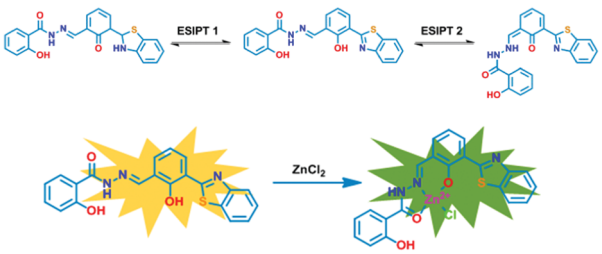

Fig. 4 Tautomers of HBS and probable binding of HBS with Zn^{2+}.

We have recorded the ^{1}H NMR spectra of the probe (HBS) with various concentrations of Zn^{2+} in DMSO-d_6. From the NMR data, it was observed that the peak arising at δ 11.81 and 13.50 ppm gradually disappears upon addition of Zn^{2+} and also the aromatic protons experienced a slight downfield shift. So this ^{1}H NMR titration study clearly established the fact that the binding of the probe with Zn^{2+} takes place *via* the two phenolic –OH protons in HBS indicating that it may undergo complexation with Zn^{2+} (Fig. S16, ESI†). The HRMS spectrum of HBS exhibits a peak at *m*/*z* 390.1196 and 412.0732 possibly for $[HBS + H]^+$ and $[HBS + Na]^+$ respectively (Fig. S12, ESI†) whereas the HBS–Zn^{2+} complex shows a peak at *m*/*z* 485.2289 and at 507.2065 which could be attributed to $[M + Zn^{2+} + Cl^- + H]^+$ and $[M + Zn^{2+} + Cl^- + Na^+ - H]^+$, respectively, which also proves the formation of a mononuclear complex of HBS and Zn^{2+} (Fig. S17, ESI†).

Dip-stick experiment: sensing of Zn^{2+} using a TLC plate

Inspired by the specific selectivity of HBS towards Zn^{2+}, we decided to bring out some potential application by using the single molecule as a handy portable tool for sensing this metal cation. This experiment has great importance as without the

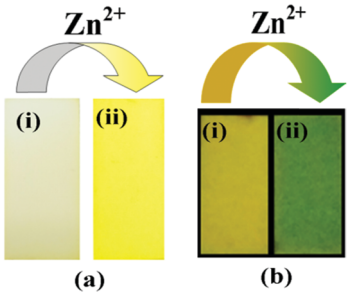

Fig. 5 Photographs of TLC plates after immersion in an HBS–MeOH solution (i) and after immersion in an HBS–Zn^{2+} methanol solution (ii) under ambient light (a) and under hand-held UV light (b). [HBS] = 2×10^{-4} M, [Zn^{2+}] = 2×10^{-3} M. Excitation wavelength of the UV light is 380 nm.

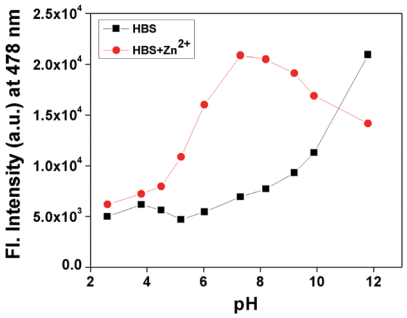

Fig. 6 Fluorescence response of HBS–Zn^{2+} as a function of pH in CH_3OH/H_2O (1/1, v/v), pH is adjusted by using aqueous solutions of 1 M HCl or 1 M NaOH.

aid of any instruments, it can give some vital qualitative information on the binding of Zn^{2+} with the receptor HBS in the solid state. In order to perform this experiment, few thin-layer chromatography (TLC) plates were prepared and immersed into HBS solution (2×10^{-4} M) in MeOH and then kept for a few minutes to evaporate the solvent, followed by dipping the TLC plates into Zn^{2+} (2×10^{-3} M) solution and then exposure to air for evaporating the solvent.

Now in the case of Zn^{2+}, the colour of the TLC plates changes from colourless to yellow in ambient light while under UV light the colour changes from yellow to green (Fig. 5). This experiment enables a real time monitoring and does not require the use of any instrumental analysis, just *via* naked-eye detection and using TLC plates we can easily perform an instant qualitative detection of Zn^{2+}.

pH study

Now the acid–base titration experiment uncovered the truth that HBS does not undergo any notable change in the emission profile at 478 nm within the pH range of 2–8. This investigation suggests that the molecule is stable in this pH range. But under strongly basic conditions ranging from pH 9 to 12, deprotonation of the phenolic hydroxyl group causes the yellow coloration along with increased fluorescence at 478 nm. In the presence of Zn^{2+} in the pH range of 4.5–9.2, the emission intensity increases and is sufficient enough for detecting Zn^{2+} while in the pH range of 10–12 the emission intensity starts to decrease (Fig. 6). Thus HBS can be used for the detection of Zn^{2+} at almost neutral pH (pH = 7.2).

Computational study

To further understand the relationship between the structural changes of HBS and its complex with Zn^{2+}, we carried out density functional theory (DFT) and time dependent density functional theory (TDDFT) calculations with the B3LYP/6-31+G(d) method basis set using the Gaussian 09 program. The optimized geometry and the highest occupied molecular orbital (HOMO) and the lowest unoccupied molecular orbital (LUMO) of HBS and its Zn^{2+} complex are presented in Fig. S13–S16 (ESI†). The HOMO–LUMO energy gap for HBS is found to be 3.72 eV which is reduced in HBS–Zn^{2+} to 3.47 eV. The generation of a new band at a longer wavelength for the HBS–Zn^{2+} complex is well correlated with the reduced HOMO–LUMO energy gap (Tables S2 and S3, ESI†).

Cell study

To evaluate the cytotoxicity of HBS and the HBS–Zn^{2+} complex a cell viability study with human breast cancer cell lines (MCF-7) was carried by the MTT method. The MTT experiment establishes that the free receptor (HBS) has a negligible toxicity at lower concentrations towards MCF-7 cell lines (Fig. S22, ESI†). To examine the fluorescence efficiency of HBS and the HBS–Zn^{2+} complex in biological samples, treated MCF-7 cells were fixed and observed under a fluorescence microscope. Our results revealed that treatment with a receptor showed a reddish fluorescence in the intracellular region of MCF-7 cells. While incubation of the cells with Zn^{2+} and HBS showed a distinct shift to green fluorescence in the same intracellular region (Fig. 7). To further confirm our study, the collected breast cancer tissue sample was incubated with HBS and the

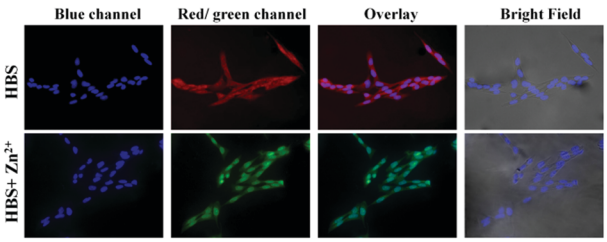

Fig. 7 Fluorescence image of MCF-7 cells after incubation with 15 μM HBS and HBS–Zn^{2+} complex. DAPI is used to stain the nucleus.

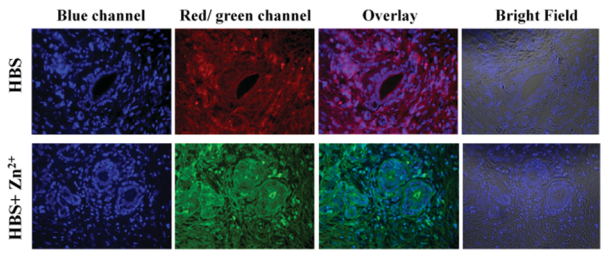

Fig. 8 Fluorescence image of human breast tissues after incubation with 15 μM HBS and HBS–Zn^{2+} complex. DAPI is used to stain the nucleus.

HBS–Zn^{2+} complex. Consistent with the cell line results from the breast cancer tissue sample that showed a reddish fluorescence with the free receptor and green fluorescence with the HBS–Zn^{2+} complex under a fluorescence microscope. Together all the results indicated that the chemosensor has the ability to penetrate the cell membrane and bind to intracellular Zn^{2+} to form a HBS–Zn^{2+} complex. DAPI was used to stain the nucleus (Fig. 8).

Conclusions

So a new fluorescence sensing switch based on hydroxybenzothiazole moieties has been successfully designed and synthesized. This newly fabricated probe utilized the ESIPT strategy to procure a highly efficient fluorescent molecular switch for selective detection of Zn^{2+}. Addition of increased concentrations of Zn^{2+} exhibits a noteworthy emission enhancement accompanied with a blue-shift in the emission maxima along with a visible colour change from colorless to light yellow. This ESIPT based fluorescent probe shows high selectivity and sensitivity towards Zn^{2+} over other respective analytes with a very low detection limit of 1.6×10^{-7} M under physiological conditions. The structure of the probe and probable binding modes with Zn^{2+} were further examined by DFT and TDDFT calculations. Also to reveal its value in practical applications, the dip-stick experiment was performed along with live cell imaging studies using human breast cancer cell lines (MCF-7) and tissues.

Conflicts of interest

There are no conflicts to declare.

Acknowledgements

The authors thank CSIR and SERB, New Delhi, India, for financial support. K. A. and D. S. thank DST-SERB for providing the N-PDF fellowships. S. G. and L. P. acknowledge UGC, New Delhi, India for providing them fellowships.

Notes and references

1 K. Rurack and U. Resch-Genger, *Chem. Soc. Rev.*, 2002, **31**, 116.
2 J. Du, M. Hu, J. Fan and X. Peng, *Chem. Soc. Rev.*, 2012, **41**, 4511.
3 I. Bertini, H. B. Gray, S. J. Lippard and J. S. Valentin, *Bioinorganic Chemistry*, University Science Books, Mill Valley, USA, 1994.
4 (*a*) J. M. Berg and Y. Shi, *Science*, 1996, **271**, 1081; (*b*) X. Xie and T. G. Smart, *Nature*, 1991, **349**, 521; (*c*) C. J. Frederickson, J.-Y. Koh and A. I. Bush, *Nat. Rev. Neurosci.*, 2005, **6**, 449.
5 E. Loisel, L. Jacquamet, L. Serre, C. Bauvois, J. L. Ferrer, T. Vernet, A. M. D. Guilmi and C. Duurmort, *J. Mol. Biol.*, 2008, **381**, 594.
6 R. A. Sperotto, T. Boff, G. L. Duarte, L. S. Santos, M. A. Grusak and J. P. Fett, *J. Plant Physiol.*, 2010, **167**, 1500.
7 D. J. Bobilya, J. T. Reynolds, K. L. Faia, M. B. Anderson and P. G. Reeves, *J. Nutr. Biochem.*, 1999, **10**, 139.
8 A. I. Bush, *Curr. Opin. Chem. Biol.*, 2000, **4**, 184.
9 (*a*) P. J. Fraker and L. E. King, *Annu. Rev. Nutr.*, 2004, **24**, 277; (*b*) C. F. Walker and R. E. Black, *Annu. Rev. Neurosci.*, 2004, **24**, 255; (*c*) D. W. Choi and J. Y. Koh, *Annu. Rev. Neurosci.*, 1998, **21**, 347; (*d*) J. H. Weiss, S. L. Sensi and J. Y. Koh, *Trends Pharmacol. Sci.*, 2000, **21**, 395.
10 S. L. Galasso and R. H. Dyck, *Mol. Med.*, 2007, **13**, 380.
11 (*a*) L. C. Costello, Y. Liu, J. Zou and R. B. Franklin, *J. Biol. Chem.*, 1999, **274**, 17499; (*b*) S. M. Henshall, D. E. H. Afar, K. K. Rasiah, L. G. Horvath, K. Gish, I. Caras, V. Ramakrishnan, M. Wong, U. Jeffry and J. G. Kench, *Oncogene*, 2003, **22**, 6005.
12 (*a*) J. Lai, A. Moxey, G. Nowak, K. Vashum, K. Bailey and M. McEvoy, *J. Affective Disord.*, 1999, **56**, 189; (*b*) J. H. Weiss, S. L. Sensi and J. Y. Koh, *Trends Pharmacol. Sci.*, 2000, **21**, 395; (*c*) M. Maes, N. D. Vos, P. Demedts, A. Wauters and H. Neels, *J. Affective Disord.*, 2012, **136**, 31.
13 (*a*) E. Zhang, E. Lui, J. Shen, Y. Cao and Y. Li, *J. Environ. Sci.*, 2012, **24**, 1189; (*b*) J. Cherif, C. Mediouni, W. B. Ammar and F. Jemal, *J. Environ. Sci.*, 2011, **23**, 837.
14 (*a*) D. B. Kevin, V. B. Mykhailo, F. Andrew, R. M. Alma, D. K. Oleksiy, A. M. Ivan, E. M. Artem and V. P. Olga, *J. Phys. Chem. B*, 2010, **114**, 9313; (*b*) H. M. Chawla, S. Richa and P. Shubha, *Tetrahedron Lett.*, 2012, **53**, 2996; (*c*) T. B. Wei, P. Zhang, B. B. Shi, P. Chen, Q. Lin, J. Liu and Y. M. Zhang, *Dyes Pigm.*, 2013, **97**, 297.
15 (*a*) E. Kimura and T. Koike, *Chem. Soc. Rev.*, 1998, **27**, 179; (*b*) P. Jiang and Z. Guo, *Coord. Chem. Rev.*, 2004, **248**, 205; (*c*) N. C. Lim, H. C. Freake and C. Bruckner, *Chem. – Eur. J.*, 2005, **11**, 38; (*d*) Z. C. Liu, B. D. Wang, Z. Y. Yang, T. R. Li and Y. Li, *Inorg. Chem. Commun.*, 2010, **13**, 606; (*e*) J. Hye Kang and C. Kim, *Photochem. Photobiol. Sci.*, 2018, **17**, 442; (*f*) A. O. Eseola, H. Görls, M. Bangesh and W. Plass, *New J. Chem.*, 2018, **42**, 7884; (*g*) F. Qu, L. Zhao, W. Han and J. You, *J. Mater. Chem. B*, 2018, **6**, 4995; (*h*) R. Purkait, S. Dey and C. Sinha, *New J. Chem.*, 2018, **42**, 16653.
16 (*a*) D. Sarkar, A. K. Pramanik and T. K. Mondal, *RSC Adv.*, 2014, **4**, 25341; (*b*) Z. Dong, X. Le, P. Zhou, C. Dong and J. Ma, *RSC Adv.*, 2014, **4**, 18270; (*c*) G. J. Park, Y. J. Na, H. Y. Jo, S. A. Lee, A. R. Kim, I. Nohb and C. Kim, *New J. Chem.*, 2014, **38**, 2587; (*d*) K. Aich, S. Goswami, S. Das and C. Das Mukhopadhyay, *RSC Adv.*, 2015, **5**, 31189; (*e*) G. R. C. Hamilton, Y. Sheng, B. Callan, R. F. Donnelly and J. F. Callan, *New J. Chem.*, 2015, **39**, 3461; (*f*) M. Sohrabi, M. Amirnasr, S. Meghdadi, M. Lutz, M. B. Torbati and H. Farrokhpour, *New J. Chem.*, 2018, **42**, 12595; (*g*) R. Selva Kumar, S. K. A. Kumar, K. Vijayakrishna, A. Sivaramakrishna, P. Paira, C. V. S. B. Rao, N. Sivaraman and S. K. Sahoo, *New J. Chem.*, 2018, **42**, 8494; (*h*) H. Liu, T. Liu, J. Li, Y. Zhang, J. Li, J. Song, J. Qu and W.-Y. Wong, *J. Mater. Chem. B*, 2018, **6**, 5435; (*i*) T. Mandal, A. Hossain, A. Dhara, A. A. Masum, S. Konar, S. K. Manna, S. K. Seth, S. Pathak and S. Mukhopadhyay, *Photochem. Photobiol. Sci.*, 2018, **17**, 1068; (*j*) Y.-S. Yang, C.-M. Ma, Y.-P. Zhang, Q.-H. Xue, J.-X. Ru, X.-Y. Liu and

H.-C. Guo, *Anal. Methods*, 2018, **10**, 1833; (*k*) E. Feng, Y. Tu, C. Fan, G. Liu and S. Pu, *RSC Adv.*, 2017, **7**, 50188.
17 A. D. Becke, *J. Chem. Phys.*, 1993, **98**, 5648.
18 C. Lee, W. Yang and R. G. Parr, *Phys. Rev. B: Condens. Matter Mater. Phys.*, 1988, **37**, 785.
19 P. J. Hay and W. R. Wadt, *J. Chem. Phys.*, 1985, **82**, 270.
20 W. R. Wadt and P. J. Hay, *J. Chem. Phys.*, 1985, **82**, 284.
21 P. J. Hay and W. R. Wadt, *J. Chem. Phys.*, 1985, **82**, 299.
22 R. Bauernschmitt and R. Ahlrichs, *Chem. Phys. Lett.*, 1996, **256**, 454.
23 R. E. Stratmann, G. E. Scuseria and M. J. Frisch, *J. Chem. Phys.*, 1998, **109**, 8218.
24 M. E. Casida, C. Jamorski, K. C. Casida and D. R. Salahub, *J. Chem. Phys.*, 1998, **108**, 4439.
25 V. Barone and M. Cossi, *J. Phys. Chem. A*, 1998, **102**, 1995.
26 M. Cossi and V. Barone, *J. Chem. Phys.*, 2001, **115**, 4708.
27 M. Cossi, N. Rega, G. Scalmani and V. Barone, *J. Comput. Chem.*, 2003, **24**, 669.
28 M. J. Frisch, G. W. Trucks, H. B. Schlegel, G. E. Scuseria, M. A. Robb, J. R. Cheeseman, G. Scalmani, V. Barone, B. Mennucci, G. A. Petersson, H. Nakatsuji, M. Caricato, X. Li, H. P. Hratchian, A. F. Izmaylov, J. Bloino, G. Zheng, J. L. Sonnenberg, M. Hada, M. Ehara, K. Toyota, R. Fukuda, J. Hasegawa, M. Ishida, T. Nakajima, Y. Honda, O. Kitao, H. Nakai, T. Vreven, J. A. Montgomery, Jr., J. E. Peralta, F. Ogliaro, M. Bearpark, J. J. Heyd, E. Brothers, K. N. Kudin, V. N. Staroverov, R. Kobayashi, J. Normand, K. Raghavachari, A. Rendell, J. C. Burant, S. S. Iyengar, J. Tomasi, M. Cossi, N. Rega, J. M. Millam, M. Klene, J. E. Knox, J. B. Cross, V. Bakken, C. Adamo, J. Jaramillo, R. Gomperts, R. E. Stratmann, O. Yazyev, A. J. Austin, R. Cammi, C. Pomelli, J. W. Ochterski, R. L. Martin, K. Morokuma, V. G. Zakrzewski, G. A. Voth, P. Salvador, J. J. Dannenberg, S. Dapprich, A. D. Daniels, Ö. Farkas, J. B. Foresman, J. V. Ortiz, J. Cioslowski and D. J. Fox, *Gaussian 09, Revision D.01*, Gaussian, Inc., Wallingford CT, 2009.
29 S. Ray, N. Murmu, J. Adhikari, S. Bhattacharyya, S. Adhikari and S. Banerjee, *J. Environ. Pathol., Toxicol. Oncol.*, 2014, **33**, 295.
30 J.-P. Costes, C. Duhayon and L. Vendier, *Inorg. Chem.*, 2014, **53**, 2181.
31 P. Xu, M. Liu, T. Gao, H. Zhang, Z. Li, X. Huang and W. Zeng, *Tetrahedron Lett.*, 2015, **56**, 4007.
32 S. Goswami, A. Manna, S. Paul, A. K. Das, K. Aich and P. K. Nandi, *Chem. Commun.*, 2013, **49**, 2912.
33 G. Karabanovich, J. Zemanová, T. Smutný, R. Székely, M. Šarkan, I. Centárová, A. Vocat, I. Pávková, P. Čonka, J. Němeček, J. Stolaříková, M. Vejsová, K. Vávrová, V. Klimešová, A. Hrabálek, P. Pávek, S. T. Cole, K. Mikušová and J. Roh, *J. Med. Chem.*, 2016, **59**, 2362.
34 S. Das, S. Goswami, K. Aich, K. Ghoshal, C. K. Quah, M. Bhattacharyya and H.-K. Fun, *New J. Chem.*, 2015, **39**, 8582.
35 S. Goswami, S. Das, K. Aich, B. Pakhira, S. Panja, S. K. Mukherjee and S. Sarkar, *Org. Lett.*, 2013, **15**, 5412.